condensed matter

Article

The Effect of an Anisotropic Scattering Rate on the Magnetoresistance of a Metal: A Cuprate-Inspired Analysis

Giovanni Mirarchi [1] and Sergio Caprara [2,3,*]

[1] Institut für Theoretische Physik und Astrophysik, Universität Würzburg, Am Hubland, 97074 Würzburg, Germany; giovanni.mirarchi@uniroma1.it
[2] Dipartimento di Fisica, Sapienza Università di Roma, Piazzale Aldo Moro 5, I-00185 Rome, Italy
[3] Consiglio Nazionale delle Ricerche—Istituto dei Sistemi Complessi, Via dei Taurini 19, I-00185 Rome, Italy
* Correspondence: sergio.caprara@roma1.infn.it

Abstract: Inspired by the phenomenology of high-critical-temperature superconducting cuprates, we investigate the effect of an anisotropic scattering rate on the magnetoresistance of a metal, relying on Chambers' solution to the Boltzmann equation. We find that if the scattering rate is enhanced near points of the Fermi surface with a locally higher density of states, an extended regime is found where the magnetoresistance varies linearly with the magnetic field. We then apply our results to fit the experimental magnetoresistance of $La_{1.6-x}Nd_{0.4}Sr_xCuO_4$ and speculate about the possible source of anisotropic scattering.

Keywords: magnetoresistance; anomalous metals; high-critical-temperature superconducting cuprates

check for updates

Citation: Mirarchi, G.; Caprara, S. The Effect of an Anisotropic Scattering Rate on the Magnetoresistance of a Metal: A Cuprate-Inspired Analysis. *Condens. Matter* **2024**, *9*, 52. https://doi.org/10.3390/condmat9040052

Academic Editor : Yoshikazu Mizuguchi

Received: 29 September 2024
Revised: 15 November 2024
Accepted: 25 November 2024
Published: 29 November 2024

1. Introduction

The anomalous properties of the metallic state of high-critical-temperature superconducting cuprates are an intensely debated subject of investigation in condensed matter physics. The most noticeable anomalies are an extended temperature range in which a linear-in-temperature electrical resistivity ($\rho(T)$) is observed [1–3]; anomalous power laws and a scaling dependence of the imaginary part of the electron self-energy ($\mathrm{Im}\,\Sigma(\omega, T) = T\mathcal{S}(\omega/T)$) [4,5], which is mirrored in a similar scaling dependence of the AC conductivity ($\sigma(\omega, T)$) [6–11], at least over a certain frequency range; a seemingly divergent specific heat coefficient (C_v/T [12]), which seems to be mirrored by a seemingly divergent carrier mass [11], as extracted by finite frequency extrapolation of the optical mass; and an extended range of magnetic fields where a linear dependence of the magnetoresistance on the magnetic field is observed [2,13].

There is no microscopic theory that captures all the above-mentioned rich phenomenology. The phenomenological theory of the marginal Fermi liquid [4] poses the scaling form of the imaginary part of the electron self-energy as a fundamental property and derives a wealth of consequences, such as a divergent quasiparticle mass, but there is not yet a microscopic model of interacting electrons that behaves as a marginal Fermi liquid. Within this respect, for instance, engineered SYK models [14,15] describing a strongly interacting quantum system with random all-to-all couplings with a large number of external degrees of freedom can be considered as effective theories. Other scenarios invoke the proximity to a quantum critical point. In these theories, the critical fluctuations near the quantum critical point couple with the electrons, endowing them with non-Fermi liquid properties. The main problem with these theories is that the most convincing candidates as quantum critical points in cuprates are associated with an ordering at finite wavelengths, i.e., a finite characteristic wave vector $\mathbf{q}_c$. These are the antiferromagnetic order [16,17], which is found in the parent insulating compound and extends to small doping [18], and charge order in the form of incommensurate charge density waves [19], for which there is now clear evidence in all families of cuprates [20]. However, the electrons that are strongly scattered by the critical fluctuations are found on the Fermi surface, at isolated spots that are connected by the a characteristic wave vector $\mathbf{q}_c$ (hot spots). All the other electrons are only weakly scattered and form a Fermi liquid that short-circuits the non-Fermi liquid transport properties of the very few hot electrons [21].

Recently, an alternative scenario was proposed in which the Fermi liquid properties gently shrink with reducing temperature as a result of the coupling of the electrons with fluctuations in the finite characteristic wave vector that are nearly (but not exactly) critical and become overdamped at low temperatures [22]. Experimental evidence for such fluctuations in cuprates was recently provided by resonant inelastic X-ray scattering (RIXS) experiments [23,24], which showed that besides nearly critical charge density waves (CDWs) characterized by a narrow peak in the spectra, charge excitations with much broader spectral features were also observed. These excitations, called charge density fluctuations (CDFs), have a characteristic wave vector $\mathbf{q}_c$ very close to the wave vector of CDWs and must, therefore, have a similar origin, although they do not show any tendency to become critical, do not compete with supercondcutivity, extend across temperature and doping ranges much broader than those in which CDWs are observed, and are robust with respect to the unidirectional suppression of CDWs in strained thin films [25]. CDFs are excitations with sufficiently low characteristic energy to be a strong source of scattering for the electrons. At the same time, being characterized by broad spectra in momentum space, they mediate a scattering that is essentially isotropic on the Fermi surface, escaping the fate of theories with hot spots. It was shown that the imaginary part of the electron self-energy resulting from the scattering mediated by CDFs resembles that of a marginal Fermi liquid, although the ω/T scaling is eventually violated due the non-critical character of CDFs, and the resulting electrical resistivity is linear in temperature above the critical superconducting temperature [26,27].

A question then arises about the transport properties in the presence of a magnetic field. Inspired by a crucial observation of the authors of Refs. [13,28] that points towards an important role of an anisotropic scattering mechanism in producing a magnetoresistance that is linear in the magnetic field over a wide range, we want to systematically investigate the magnetotransport properties of electrons in the presence of a scattering rate that is anisotropic along the Fermi surface. By following the theoretical framework outlined in Refs. [13,28], we calculate the magnetoresistance, exploring its dependence on the various model parameters in wider ranges than those documented in the original works. We also provide more detail about the numerical implementation of Chambers' solution to the Boltzmann equation when applied to cuprates and derive explicit formulas for the harmonic analysis of the anisotropic component of the scattering rate. We do not make any assumption about the origin and nature of such an anisotropic scattering and limit ourselves to discussing the physical interpretation of how the parameters influence the magnetoresistance in this model. We also performed a fit of experimental data, which turned out to be consistent with our previous fits of the temperature dependence of the resistance—within our model, relying on CDFs [26,27]. This study is a preliminary but necessary step towards any attempt to incorporate CDFs into the theory of magnetotransport in cuprates, and the consistency with our previous resistivity fit is encouraging for these purposes. In the concluding part of this piece of work, we speculate about the possible source of anisotropic scattering and its connection to nearly-frozen CDF domains.

2. Dependence of the Conductivity Tensor on the Magnetic Field

In order to calculate the dependence of electrical conductivity on the magnetic field, we adopt a semiclassical approach within the framework of Boltzmann transport theory. Having in mind the case of high-T_c superconducting cuprates as a case study, our calculation applies to a layered system with tetragonal symmetry (for which we set the lattice spacing to 1), which we specialize to the case of a magnetic field perpendicular to the layers. The conductivity tensor for such a system, in the presence of a transverse magnetic field, is a 2×2 matrix such that the two diagonal components are equal to each other, as are the two off-diagonal components. Therefore, the conductivity tensor is determined only by the two diagonal and off-diagonal components, which we indicate as σ_{xx} and σ_{xy}, respectively. To determine the dependence of the magnetic field of these two quantities without any a priori assumption about the ratio between the scattering rate and the cyclotron frequency, we rely on Chambers' solution to the Boltzmann equation [29]:

$$\begin{aligned}\sigma_{xx}(B) &= \frac{2e^2}{v_{\mathrm{uc}}}\oint_{FS} v_{\mathbf{k}_{\mathrm{F}}(0),x}\left(\int_{-\infty}^{0} \mathrm{e}^{-\int_t^0 \frac{dt'}{\tau(\mathbf{k}_{\mathrm{F}}(t'))}}\,\frac{v_{\mathbf{k}_{\mathrm{F}}(t),x}}{v_{\mathbf{k}_{\mathrm{F}}(t)}}\,dt\right)\frac{dk}{4\pi^2},\\ \sigma_{xy}(B) &= \frac{2e^2}{v_{\mathrm{uc}}}\oint_{FS} v_{\mathbf{k}_{\mathrm{F}}(0),x}\left(\int_{-\infty}^{0} \mathrm{e}^{-\int_t^0 \frac{dt'}{\tau(\mathbf{k}_{\mathrm{F}}(t'))}}\,\frac{v_{\mathbf{k}_{\mathrm{F}}(t),y}}{v_{\mathbf{k}_{\mathrm{F}}(t)}}\,dt\right)\frac{dk}{4\pi^2},\end{aligned} \tag{1}$$

where e is the absolute value of the electron charge, B is the z component of the transverse magnetic field ($\mathbf{B}$), $v_{\mathbf{k}}$ is the magnitude of the electron group velocity ($\mathbf{v}_{\mathbf{k}} := \nabla_{\mathbf{k}}\xi_{\mathbf{k}}$, where $\xi_{\mathbf{k}}$ is the electron band dispersion law); while $v_{\mathbf{k},x}$ and $v_{\mathbf{k},y}$ instead to the two components of $\mathbf{v}_{\mathbf{k}}$ (we set $\hbar = 1$). The quantity denoted by v_{uc} is the volume of the three-dimensional unit cell of the layered system, so according to our units, it is simply the inter-layer distance of the in-plane lattice spacing in units. This quantity plays no role in our further calculations. Since our goal is to evaluate how the scattering anisotropy along the Fermi surface can affect the magnetotransport properties of the system, we consider an angle-dependent elastic scattering rate that does not violate the tetragonal symmetry of the system. In particular, we adopt a scattering rate of the same form as that proposed in Refs. [13,28]:

$$\frac{1}{\tau(\mathbf{k}_{\mathrm{F}})} = \frac{1}{\tau_{\mathrm{is}}} + \frac{1}{\tau_{\mathrm{an}}}|\cos(2\phi_{\mathbf{k}_{\mathrm{F}}})|^{\nu}, \tag{2}$$

where $\phi_{\mathbf{k}_{\mathrm{F}}}$ denotes the angle that the Fermi surface vector ($\mathbf{k}_{\mathrm{F}}$) makes with the positive x semiaxis in the first Brillouin zone. In our analysis, we do not study the behavior of the conductivity as a function of temperature; therefore, we do not need to separate the elastic and inelastic components in the scattering rates ($1/\tau_{\mathrm{is}}$ and $1/\tau_{\mathrm{an}}$). It is worthwhile pointing out that in this piece of work, we do not address the microscopic origin of the scattering-rate anisotropy. One possible scenario is linked to the proximity to a Van Hove singularity, which would cause an increase in the angle-dependent electron density of states. According to this view, the value of ν regulates the profile of this anisotropy.

The dependence on the magnetic field in Equation (1) comes into play through the time evolution of vector $\mathbf{k}_{\mathrm{F}}(t)$. This time evolution is governed by the standard equation of motion for an electron in a uniform electric and magnetic field:

$$\frac{d\mathbf{k}}{dt} = -e\big(\mathbf{E} + \mathbf{v}_{\mathbf{k}} \times \mathbf{B}\big). \tag{3}$$

where $\mathbf{k}$, $\mathbf{E}$, and $\mathbf{v}_{\mathbf{k}}$ lie on the lattice plane, while $\mathbf{B}$ is orthogonal. However, since we are not interested in nonlinear effects in the electrostatic field, we can set $\mathbf{E} = \mathbf{0}$ at this level. It is worth noting that, according to the system of units we are using, the quantity eB is dimensionless. In fact, the magnetic field B can be conveniently expressed in units of $B_0 := \hbar/(e\,a^2)$ (where a is the in-plane lattice spacing), which is equal to $1/e$ in our units. We define the magnetoresistance such that it vanishes at $B = 0$:

$$\mathrm{MR}(B) := \frac{\sigma_{xx}(0)}{\sigma_{xx}(B)} - 1.$$

Our main goal is to show how the magnetoresistance depends on the three scattering-rate parameters appearing in Equation (2), namely $1/\tau_{\mathrm{is}}$, $1/\tau_{\mathrm{an}}$, and ν. The band dispersion of the electron system under study is that given by tight binding, for which we only consider the first three hopping parameters:

$$\xi_{\mathbf{k}} = -2t\big[\cos(k_x) + \cos(k_y)\big] - 4t'\cos(k_x)\cos(k_y) - 2t''\big[\cos(2k_x) + \cos(2k_y)\big] - \mu.$$

The chemical potential μ is adjusted to fix the number of electrons per unit cell $(1-p)$. Details about the solution of Equation (3) to be incorporated in Equation (1), as well as a Fourier analysis of the scattering rate in Equation (2), are provided in the Appendices A and B.

3. Effect of Anisotropic Scattering

In this study, we fix the following set of parameters:

$$t = 200\,\text{meV}, \qquad t' = -0.135\,t = -27\,\text{meV},$$
$$t'' = 0.065\,t = 13\,\text{meV}, \qquad p = 0.248.$$

This set is quite similar to that proposed in Refs. [13,28]. The first problem we face is how the magnetoresistance is affected by the isotropic component of the scattering. In order to estimate the overall contributions of the two terms that make up our scattering rate, we can average the total scattering rate over a full (2π) angle:

$$\frac{1}{\tau_{\text{avg}}} := \frac{1}{2\pi}\int_0^{2\pi}\frac{d\phi_{\mathbf{k}_\text{F}}}{\tau(\mathbf{k}_\text{F})} = \frac{1}{\tau_{\text{is}}} + \frac{1}{\tau_{\text{an}}}f(\nu), \qquad \text{with} \quad f(\nu) := \frac{\Gamma\left(\frac{\nu+1}{2}\right)}{\sqrt{\pi}\,\Gamma\left(\frac{\nu}{2}+1\right)},$$

where $\Gamma(z)$ is the Euler Gamma function. The dimensionless function $f(\nu)$ is a strictly decreasing function of ν for non-negative values of its argument such that it is equal to 1 when $\nu = 0$, and has asymptotic behavior $1/\sqrt{\nu}$ for $\nu \to \infty$. In the absence of a magnetic field, if the total scattering is dominated by a single characteristic scattering rate, Boltzmann transport theory predicts a resistivity that is essentially linear. The addition of an external magnetic field generally provides a subleading correction to this dependence. For this reason, we expect the quantity of $\text{MR}(B)$, beyond its dependence on the magnetic field B, to be essentially linear in τ_{avg} due to the presence of $\rho_{xx}(0)$ in the denominator. The trend of magnetoresistance as a function of B for several values of $1/\tau_{\text{is}}$ is shown in Figure 1. All the curves in the figure exhibit a crossover between a quadratic and a linear regime, and the scale at which this crossover occurs increases with $1/\tau_{\text{is}}$. We also observe that the value of the magnetoresistance increases as τ_{is} increases according to an approximately linear relationship at high magnetic fields. It is worth noting that with the values we set for the anisotropic part of the scattering ($1/\tau_{\text{an}} = 42\,\text{meV}$ and $\nu = 12$) and with the range we chose for the isotropic one (between 3 meV and 12 meV), the quantity of $1/\tau_{\text{avg}}$ is dominated by its isotropic component, which is the reason why the linearity between $\text{MR}(B)$ and $1/\tau_{\text{avg}}$ roughly reduces to a linearity between $\text{MR}(B)$ and $1/\tau_{\text{is}}$.

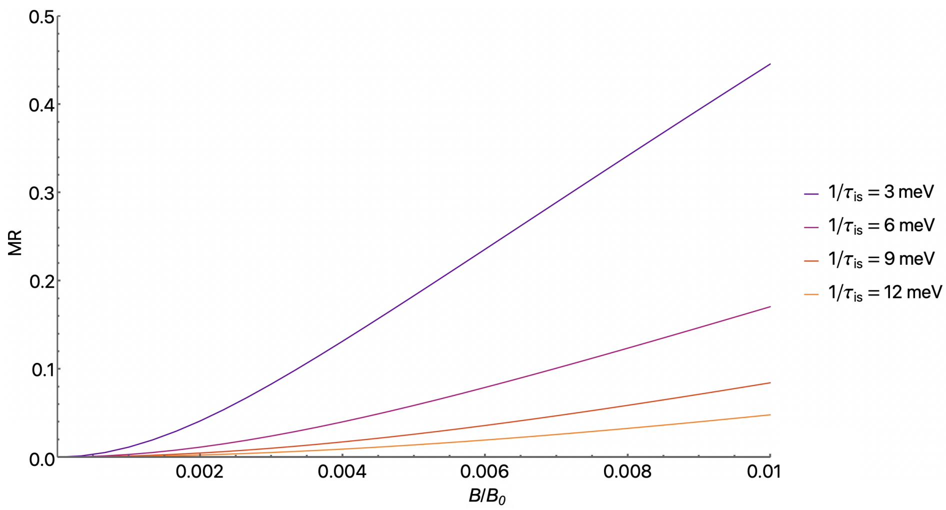

Figure 1. Magnetoresistance as a function of B for several values of $1/\tau_{\text{is}}$ at fixed $1/\tau_{\text{an}} = 42\,\text{meV}$ and $\nu = 12$.

Let us now analyze the effect of the anisotropic component of the scattering, namely how $\mathrm{MR}(B)$ is influenced by the two parameters of $1/\tau_{\mathrm{an}}$ and ν. We first observe that these two parameters play different roles within the expression for $1/\tau(\mathbf{k}_{\mathrm{F}})$: while $1/\tau_{\mathrm{an}}$ controls the relative weight between the isotropic and anisotropic parts of the scattering rate, ν determines the shape of the anisotropic part in a non-trivial way. Indeed, the the ν parameter appears in the expression for the scattering rate, i.e., Equation (2), as the exponent of $|\cos(2\phi_{\mathbf{k}_{\mathrm{F}}})|$, so it does not produce, e.g., an overall amplification or a rigid shift. Therefore, we expect that the effect of varying $1/\tau_{\mathrm{an}}$ is somewhat similar to that of varying $1/\tau_{\mathrm{is}}$, with the main difference being that the dependence of the magnetoresistance on the former is significantly weaker than that on the latter for large enough values of ν, as its contribution is significantly suppressed by factor $f(\nu)$. These observations are confirmed by our numerical calculation, the plot of which is shown in Figure 2. An important qualitative difference relative to Figure 1 is that in the second case, the curves seem to grow as $1/\tau_{\mathrm{an}}$ increases. The reason is that the scattering rate $(1/\tau_{\mathrm{an}})$ has a much weaker effect on $\rho_{xx}(0)$ than $1/\tau_{\mathrm{is}}$—weak enough to allow for the increase in resistivity due to the magnetic field to (slightly) outweigh the increase in zero-field resistance.

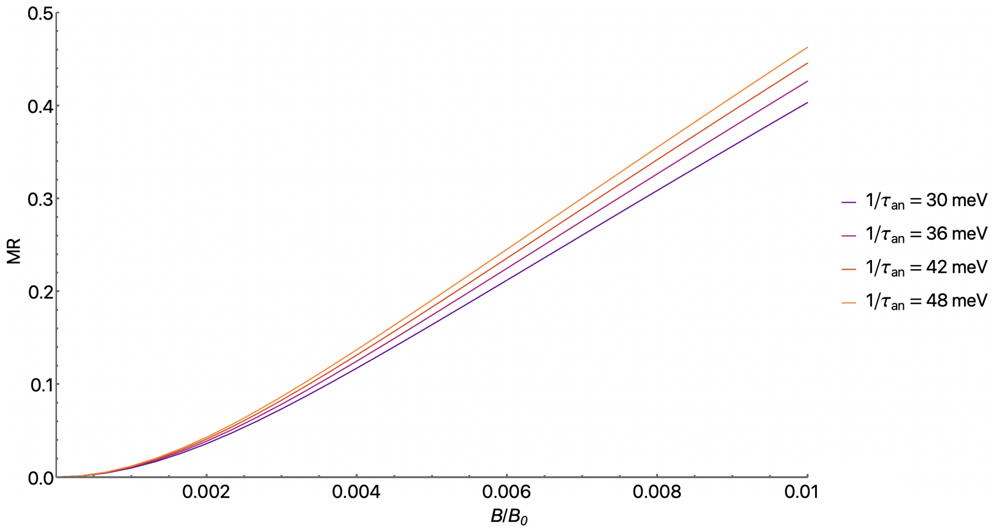

Figure 2. Magnetoresistance as a function of B for several values of $1/\tau_{\mathrm{an}}$ at fixed $1/\tau_{\mathrm{is}} = 3\,\mathrm{meV}$ and $\nu = 12$.

More interesting is the effect of varying the value of ν, which is graphically reported in Figure 3. As we have already mentioned, the increase in ν leads, on the one hand, to a sharper anisotropy of the scattering rate, but, on the other hand, it attenuates the contribution of the anisotropic component compared to the isotropic one. This is why the increase in ν has an effect somewhat opposite to that of the increase in $1/\tau_{\mathrm{an}}$, as is evidenced by comparing Figures 2 and 3. The most interesting aspect of this plot, in contrast to what we observed in Figures 1 and 2, is that the linear parts of the curves appear to have essentially the same slope and are, therefore, distinguished from each other mainly by the scale at which the crossover between the quadratic and linear regimes occurs. In particular, linearity appears to be more extended as ν decreases. However, for excessively low values of ν a deviation from linearity is observed at high magnetic fields, in favor of a sublinear trend.

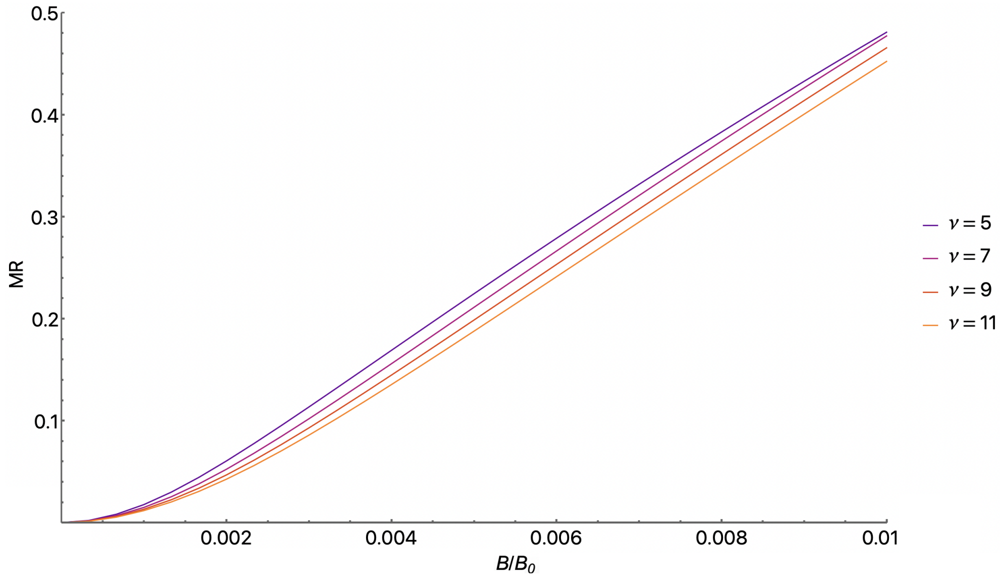

Figure 3. Magnetoresistance as a function of B for several values of ν at fixed $1/\tau_{\mathrm{is}} = 3\,\mathrm{meV}$ and $1/\tau_{\mathrm{an}} = 42\,\mathrm{meV}$.

4. Discussion and Conclusions

For the sake of concreteness, for comparison with experimental data, we adopt the same set of parameters that we already used to fit the resistivity data for $La_{1.6-x}Nd_{0.4}Sr_xCuO_4$ [27,30], whose experimental estimate is provided in Ref. [31]:

$$t = 435\,\mathrm{meV}, \qquad t' = -50\,\mathrm{meV}, \qquad t'' = 38\,\mathrm{meV}, \qquad p = 0.24.$$

With this set of parameters, we obtain $\mu \simeq -350\,\mathrm{meV}$. Moreover, in order to perform a direct comparison with the experimental data, it is necessary to express the magnetic field in standard SI units. For this reason, it is necessary to fix the value of a and, consequently, that of B_0. By setting $a = 3.8$ Å [32,33], we obtain $B_0 \simeq 4.56 \times 10^3$ T. The fit of the experimental data, as shown in Figure 4, provides the following set of values:

$$\frac{1}{\tau_{\mathrm{is}}} = 17.7\,\mathrm{meV}, \qquad \frac{1}{\tau_{\mathrm{an}}} = 39\,\mathrm{meV}, \qquad \nu = 4.$$

The explicit expression of Equation (2) for $\nu = 4$ is

$$\frac{1}{\tau(\mathbf{k}_{\mathrm{F}})} = \frac{1}{\tau_{\mathrm{is}}} + \frac{1}{\tau_{\mathrm{an}}}\left[\frac{3}{8} + \frac{1}{2}\cos(4\phi_{\mathbf{k}_{\mathrm{F}}}) + \frac{1}{8}\cos(8\phi_{\mathbf{k}_{\mathrm{F}}})\right].$$

The set of parameters we chose not only allows for a good fit of the experimental magnetoresistance curve but is also consistent with our previous fit for the resistivity data [27,30]. In fact, the value of $\rho_{xx}(0)$ that we obtain with the expression for $1/\tau(\mathbf{k}_{\mathrm{F}})$ given by (2) with the chosen parameters is the same as that obtained by setting $1/\tau(\mathbf{k}_{\mathrm{F}})$ equal to the constant value of $2\Gamma_0$ with $\Gamma_0 = 13.7\,\mathrm{meV}$, which is the value we set to fit $La_{1.6-x}Nd_{0.4}Sr_xCuO_4$ resistivity data in the absence of a magnetic field. This is a preliminary test of consistency within our attempt to formulate a theory of the strange metallic behavior of cuprates in terms of overdamped collective excitations [26,27], which is currently underway. We notice, in passing, that the extended linear behavior as a function of B is obtained here for a scattering rate that is rather less anisotropic than that suggested in Ref. [13]. Another important consequence of the mechanism underlying an extended linear dependence of the magnetoresistance on the magnetic field discussed in this piece of work is the temperature and magnetic field entering the theory in independent manners, so there is no reason to expect B/T scaling of the magnetoresistance. Of course, if the overall inverse scattering time ($1/\tau$) is directly proportional to T, then we observe a B/T scaling, as the coefficient C in the relation expressed as $\mathrm{MR}(B) = C\,B$ is proportional to τ. However, within our approach, the microscopic origins of the B linearity of the magnetoresistance and the T linearity of the scattering rate are completely unrelated to each other. The first of the two is determined by several factors, including the degree of anisotropy of the scattering on the Fermi surface, while the second is likely due to the semiclassical behavior of the collective degrees of freedom that mediate this scattering whenever the temperature is higher than the characteristic energy scale of these degrees of freedom [26,27]. This implies, for example, that the energy scales at which the linear-to-quadratic crossover is observed, both in the B dependence and in the T dependence, are unrelated, barring an accidental coincidence. Therefore, if the mechanism for the linear-in-B magnetoresistance is the one discussed in this piece of work, any observed B/T scaling is to be considered approximate or accidental.

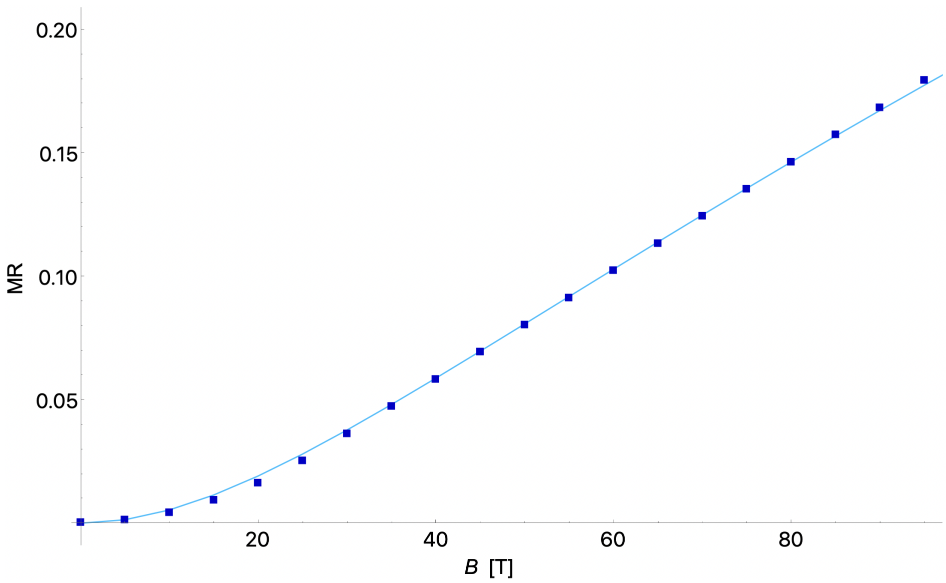

Figure 4. Plots of the experimental magnetoresistance data (dots) and theoretical fit (solid line) for $La_{1.6-x}Nd_{0.4}Sr_xCuO_4$ at $p = 24\%$ and $T = 30\,\mathrm{K}$. The experimental data are taken from Ref. [13].

So far, we have limited ourselves to identifying the range of parameters that are apt to describe the magnetoresistance of cuprates. The task of incorporating CDFs in the theory is beyond the scope of this piece of work, as it requires specifying the elastic and anelastic contributions for in both $1/\tau_{\mathrm{is}}$ and $1/\tau_{\mathrm{an}}$, with the latter governing the temperature dependence of the transport properties, which will be the subject of future investigations. However, here, we wish to speculate about the possible source of anisotropic scattering and its connection to CDFs.

To extend the linear-in-temperature electrical resistivity down to very low temperatures, as observed in cuprates when superconductivity is suppressed by a magnetic field, we were recently led to consider a theory in which the damping of CDFs increases with the lowering of the temperature and diverges at $T = 0$ (at a specific doping or in some doping range) [27,30]. Indeed, this theory allows for the extension of the linear temperature dependence of the resistivity to low temperatures. Furthermore, the electrons coupled to these overdamped CDFs form a shrinking Fermi liquid [22] that reproduces most of the phenomenology of the marginal Fermi liquid, with the important difference of yielding a quasiparticle mass that stays finite. Instead, the divergent specific heat coefficient (C_v/T) is obtained as a direct contribution of overdamped CDFs. When trying to identify the source of this overdamping, one is led to consider some kind of incipient glassy behavior for the CDFs, following an approach inspired to Ref. [34]. It is then tempting to imagine that some elongated nanoscopic CDF domains become prematurely frozen and contribute to the elastic part of the anisotropic scattering rate responsible for the linear magnetoresistance, whereas the remaining dynamical overdamped CDFs contribute to the inelastic part of the isotropic scattering rate responsible for the linear-in-temperature resistivity. This scenario is currently under investigation.

Author Contributions: Conceptualization, G.M. and S.C.; methodology, G.M. and S.C.; software, G.M.; validation, G.M. and S.C.; formal analysis, G.M. and S.C.; investigation, G.M. and S.C.; writing—original draft preparation, G.M. and S.C.; writing—review and editing, G.M. and S.C.; supervision, S.C.; funding acquisition, S.C. All authors have read and agreed to the published version of the manuscript.

Funding: We acknowledge financial support from the Ateneo Research Projects of the University of Rome Sapienza: Competing phases and non-equilibrium phenomena in low-dimensional systems with microscopic disorder and nanoscale inhomogeneities (n. RM12117A4A7FD11B), Models and theories from anomalous diffusion to strange-metal behavior (n. RM12218162CF9D05), and Non-conventional aspects for transport phenomena and non-equilibrium statistical mechanics (n. RM123188E830D258).

Data Availability Statement: No new data were created in this study. The theoretical curves presented in the various figures have been numerically calculated, based on the formulas given in the text. The experimental data fitted in Figure 4 are taken from Ref. [13].

Acknowledgments: We acknowledge fruitful conversations with M. Grilli and G. Seibold.

Conflicts of Interest: The authors declare no conflicts of interest.

Abbreviations

The following abbreviations are used in this manuscript:

CDFs	Charge density fluctuations
CDWs	Charge density waves
RIXS	Resonant Inelastic X-ray Scattering

Appendix A. Equation of Motion of an Electron in a Transverse Magnetic Field

We calculate the conductivity tensor by neglecting nonlinear effects in the electric field but keeping the full dependence on the magnetic field (at least for magnetic fields low enough to apply a semiclassical approach). Therefore, the equation of motion for the electron is obtained by setting $\mathbf{E} = \mathbf{0}$ in Equation (3):

$$\frac{d\mathbf{k}}{dt} = -\mathbf{v_k} \times e\mathbf{B}.$$

This equation can be expressed either in Cartesian coordinates (k_x, k_y) or in polar coordinates (k, ϕ) as follows:

$$\begin{cases} \dfrac{dk_x}{dt} = -eBv_y, \\[2ex] \dfrac{dk_y}{dt} = eBv_x, \end{cases} \qquad \begin{cases} \dfrac{1}{k}\dfrac{dk}{dt} = -eB\dfrac{k_x v_y - k_y v_x}{k_x^2 + k_y^2}, \\[2ex] \dfrac{d\phi}{dt} = eB\dfrac{k_x v_x + k_y v_y}{k_x^2 + k_y^2}, \end{cases}$$

where, in the last two equations, $k_x = k\cos\phi$ and $k_y = k\sin\phi$. Since the integral that defines the electrical conductivity is restricted to the Fermi surface, the various wave vectors that appear are uniquely identified by their angle with respect to the positive x semiaxis of the first Brillouin zone. Consequently, the only relevant equation of motion is the one for ϕ. Once ϕ is found, the corresponding k is adjusted so that $\mathbf{k}$ is on the Fermi surface. We point out that the angular variable ϕ varies continuously along the entire Fermi surface only if it is closed around the Γ point, namely when it crosses both axes of the first Brillouin zone, i.e., $k_x = 0$ and $k_y = 0$. For the case of an open Fermi surface, it is convenient to work with the angular variable φ, which is defined as the angle taken from the M point starting from the negative y semiaxis and taken as positive if oriented clockwise (see Figure A1). The equation of motion for φ is then

$$\frac{d\varphi}{dt} = eB\frac{\left[\pi - \left(k_x + 2\pi\theta(-k_x)\right)\right]v_x + \left[\pi - \left(k_y + 2\pi\theta(-k_y)\right)\right]v_y}{\left[\pi - \left(k_x + 2\pi\theta(-k_x)\right)\right]^2 + \left[\pi - \left(k_y + 2\pi\theta(-k_y)\right)\right]^2},$$

where $\theta(\cdot)$ is the Heaviside step function. The quantity of $k_j + 2\pi\theta(-k_j)$ (with $j = x, y$ and $k_j \in [-\pi, \pi]$) can be interpreted as a Fermi surface vector if the Fermi surface is traced around the M point instead of around the Γ point. Also notice that the sign of $\left[\pi - \left(k_j + 2\pi\theta(-k_j)\right)\right]$ is the same as that of k_j; this implies that the sign of $d\phi/dt$ is the same as that of $d\varphi/dt$, as expected. Moreover, we point out that all the functions in this expression are well defined, since in the case of an open Fermi surface with tetragonal symmetry, neither k_x nor k_y can ever vanish.

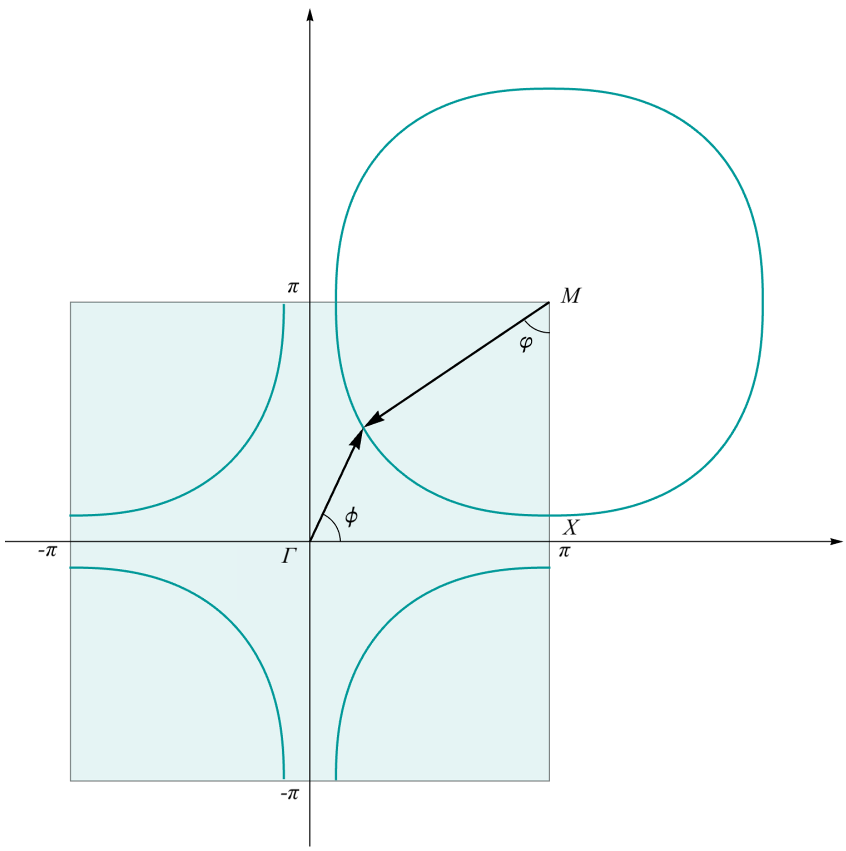

Figure A1. Graphical display of angles ϕ and φ for an open Fermi surface.

Appendix B. Harmonic Analysis of the Anisotropic Component of the Scattering Rate

The Fourier series expansion of the function expressed as $|\cos(2\phi)|^{\nu}$ provides the following result:

$$|\cos(2\phi)|^{\nu} = \frac{1}{2}a_0 + \sum_{n=1}^{\infty} a_n \cos(4n\phi),$$

where

$$a_n = \frac{\Gamma(\nu+1)\Gamma\left(n - \frac{\nu}{2}\right)}{2^{\nu-1}\pi\Gamma\left(n + 1 + \frac{\nu}{2}\right)} \cos\left[\left(n + \frac{\nu+1}{2}\right)\pi\right].$$

This is a quite general expression that works for any real $\nu \geq 0$. Notice the following asymptotic behavior:

$$\frac{\Gamma\left(n-\frac{\nu}{2}\right)}{\Gamma\left(n+1+\frac{\nu}{2}\right)} \sim \frac{1}{n^{\nu+1}} \qquad \text{for} \quad n \to \infty,$$

which ensures that the previous series is always convergent for any $\nu > 0$. A very interesting expression can be found when ν is an even, non-negative integer. In this case, we can express it as $2m$, where $m \in \mathbb{N}_0$. The expression for a generic coefficient a_n is

$$a_n = \begin{cases} 2^{1-2m}\dbinom{2m}{m-n} & \text{for } 0 \leq n \leq m, \\ 0 & \text{for } n > m, \end{cases}$$

which shows that only a finite number of harmonics contributes to the reconstruction of the original function, as required by appropriate trigonometric identities. In particular, for the trivial case of $\nu = m = 0$, the only non-zero term is $a_0 = 2$, as expected, since in this case, our function becomes constant.

References

1. Dagotto, E. Correlated electrons in high-temperature superconductors. *Rev. Mod. Phys.* **1994**, *66*, 763–840. [CrossRef]
2. Giraldo-Gallo, P.; Galvis, J.A.; Stegen, Z.; Modic, K.A.; Balakirev, F.F.; Betts, J.B.; Lian, X.; Moir, C.; Riggs, S.C.; Wu, J.; et al. Scale-invariant magnetoresistance in a cuprate superconductor. *Science* **2018**, *361*, 479–481. [CrossRef] [PubMed]
3. Legros, A.; Benhabib, S.; Tabis, W.; Laliberté, F.; Dion, M.; Lizaire, M.; Vignolle, B.; Vignolles, D.; Raffy, H.; Li, Z.Z.; et al. Universal T-linear resistivity and Planckian dissipation in overdoped cuprates. *Nat. Phys.* **2019**, *15*, 142. [CrossRef]
4. Varma, C.M.; Littlewood, P.B.; Schmitt-Rink, S.; Abrahams, E.; Ruckenstein, A.E. Phenomenology of the normal state of Cu-O high-temperature superconductors. *Phys. Rev. Lett.* **1989**, *63*, 1996. [CrossRef]
5. Damascelli, A.; Hussain, Z.; Shen, Z.-X. Angle-resolved photoemission studies of the cuprate superconductors . *Rev. Mod. Phys.* **2003**, *75*, 473. [CrossRef]
6. El Azrak, A.; Nahoum, R.; Bontemps, N.; Guilloux-Viry, M.; Thivet, C.; Perrin, A.; Labdi, S.; Li, Z.Z.; Raffy, H. Infrared properties of $YBa_2Cu_3O_7$ and $Bi_2Sr_2Ca_{n-1}Cu_nO_{2n+4}$ thin films. *Phys. Rev. B* **1994**, *49*, 9846. [CrossRef]
7. van der Marel, D.; Molegraaf, H.J.A.; Zaanen, J.; Nussinov, Z.; Carbone, F.; Damascelli, A.; Eisaki, H.; Greven, M.; Kes, P.H.; Li, M. Quantum critical behaviour in a high-T_c superconductor. *Nature* **2003**, *425*, 271. [CrossRef]
8. van der Marel, D.; Carbone, F.; Kuzmenko, A.B.; Giannini, E. Scaling properties of the optical conductivity of Bi-based cuprates. *Ann. Phys.* **2006**, *321*, 1716.
9. Hwang, J.; Timusk, T.; Gu, G.D. Doping dependent optical properties of $Bi_2Sr_2CaCu_2O_{8+\delta}$. *J. Phys. Condens. Matter* **2007**, *19*, 125208. [CrossRef]
10. van Heumen, E.; Feng, X.; Cassanelli, S.; Neubrand, L.; de Jager, L.; Berben, M.; Huang, Y.; Kondo, T.; Takeuchi, T.; Zaanen, J. Strange metal electrodynamics across the phase diagram of $Bi_{2-x}Pb_xSr_{2-y}La_yCuO_{6+\delta}$ cuprates. *Phys. Rev. B* **2022**, *106*, 054515. [CrossRef]
11. Michon, B.; Berthod, C.; Rischau, C.W.; Ataei, A.; Chen, L.; Komiya, S.; Ono, S.; Taillefer, L.; van der Marel, D.; Georges, A. Reconciling scaling of the optical conductivity of cuprate superconductors with Planckian resistivity and specific heat. *Nat. Commun.* **2023**, *14*, 3033. [CrossRef] [PubMed]
12. Michon, B.; Girod, C.; Badoux, S.; Kačmarčík, J.; Ma, Q.; Dragomir, M.; Dabkowska, H.A.; Gaulin, B.D.; Zhou, J.S.; Pyon, S.; et al. Thermodynamic signatures of quantum criticality in cuprate superconductors. *Nature* **2019**, *567*, 218–222. [CrossRef] [PubMed]
13. Ataei, A.; Gourgout, A.; Grissonnanche, G.; Chen, L.; Baglo, J.; Boulanger, M.-E.; Laliberté, F.; Badoux, S.; Doiron-Leyraud, N.; Oliviero, V.; et al. Electrons with Planckian scattering obey standard orbital motion in a magnetic field. *Nat. Phys.* **2022**, *18*, 1420–1424. [CrossRef]
14. Chowdhury, D.; Werman, Y.; Berg, E.; Senthil, T. Translationally Invariant Non-Fermi-Liquid Metals with Critical Fermi Surfaces: Solvable Models. *Phys. Rev. X* **2018**, *8*, 031024. [CrossRef]
15. Patel, A.A.; McGreevy, J.; Arovas, D.P.; Sachdev, S. Magnetotransport in a Model of a Disordered Strange Metal. *Phys. Rev. X* **2018**, *8*, 021049. [CrossRef]
16. Chakravarty, S.; Halperin, B.I.; Nelson, D.R. Low-temperature behavior of two-dimensional quantum antiferromagnets. *Phys. Rev. Lett.* **1988**, *60*, 1057. [CrossRef] [PubMed]
17. Lee, P.A.; Nagaosa, N.; Wen, X. Doping a Mott Insulator: Physics of High Temperature Superconductivity. *Rev. Mod. Phys.* **2006**, *78*, 17–85. [CrossRef]

18. Vaknin, D.; Sinha, S.K.; Moncton, D.E.; Johnston, D.C.; Newsam, J.M.; Safinya, C.R.; King, H.E., Jr. Antiferromagnetism in La_2CuO_{4-y}. *Phys. Rev. Lett.* **1987**, *58*, 2802. [CrossRef]
19. Castellani, C.; Di Castro, C.; Grilli, M. Singular Quasiparticle Scattering in the Proximity of Charge Instabilities. *Phys. Rev. Lett.* **1995**, *75*, 4650. [CrossRef]
20. Arpaia, R.; Ghiringhelli, G. Charge Order at High Temperature in Cuprate Superconductor. *J. Phys. Soc. Jpn.* **2021**, *90*, 111005. [CrossRef]
21. Hlubina, R.; Rice, T.M. Resistivity as a function of temperature for models with hot spots on the Fermi surface. *Phys. Rev. B* **1995**, *51*, 9253. [CrossRef] [PubMed]
22. Mirarchi, G.; Grilli, M.; Seibold, G.; Caprara, S. The Shrinking Fermi Liquid Scenario for Strange-Metal Behavior from Overdamped Optical Phonons. *Condens. Matter* **2024**, *9*, 14. [CrossRef]
23. Arpaia, R.; Caprara, S.; Fumagalli, R.; De Vecchi, G.; Peng, Y.Y.; Andersson, E.; Betto, D.; De Luca, G.M.; Brookes, N.B.; Lombardi, F.; et al. Dynamical charge density fluctuations pervading the phase diagram of a Cu-based high-Tc superconductor. *Science* **2019**, *365*, 906. [CrossRef] [PubMed]
24. Arpaia, R.; Martinelli, L.; Sala, M.M.; Caprara, S.; Nag, A.; Brookes, N.B.; Camisa, P.; Li, Q.; Gao, Q.; Zhou, X.; et al. Signature of quantum criticality in cuprates by charge density fluctuations. *Nat. Commun.* **2023**, *14*, 7198. [CrossRef] [PubMed]
25. Wahlberg, E.; Arpaia, R.; Seibold, G.; Rossi, M.; Fumagalli, R.; Trabaldo, E.; Brookes, N.B.; Braicovich, L.; Caprara, S.; Gran, U.; et al. Restored strange metal phase through suppression of charge density waves in underdoped $YBa_2Cu_3O_{7-\delta}$. *Science* **2021**, *373*, 1506. [CrossRef]
26. Seibold, G.; Arpaia, R.; Peng, Y.Y.; Fumagalli, R.; Braicovich, L.; Di Castro, C.; Grilli, M.; Ghiringhelli, G.C.; Caprara, S. Strange metal behaviour from charge density fluctuations in cuprates. *Commun. Phys.* **2021**, *4*, 7. [CrossRef]
27. Mirarchi, G.; Seibold, G.; Castro, C.D.; Grilli, M.; Caprara, S. The strange-metal behavior of cuprates. *Condens. Matter* **2022**, *7*, 29. [CrossRef]
28. Grissonnanche, G.; Fang, Y.; Legros, A.; Verret, S.; Laliberté, F.; Collignon, C.; Zhou, J.; Graf, D.; Goddard, P.A.; Taillefer, L.; et al. Linear-in-temperature resistivity from an isotropic Planckian scattering rate. *Nature* **2021**, *595*, 667–672. [CrossRef]
29. Chambers, R.G. The Kinetic Formulation of Conduction Problems. *Proc. Phys. Soc. A* **1952**, *65*, 458. [CrossRef]
30. Caprara, S.; Castro, C.D.; Mirarchi, G.; Seibold, G.; Grilli, M. Dissipation-driven strange metal behavior. *Commun. Phys.* **2022**, *5*, 10. [CrossRef]
31. Meevasana, W.; Zhou, X.J.; Sahrakorpi, S.; Lee, W.S.; Yang, W.L.; Tanaka, K.; Mannella, N.; Yoshida1, T.; Lu, D.H.; Chen, Y.L.; et al. Hierarchy of multiple many-body interaction scales in high-temperature superconductors. *Phys. Rev. B* **2007**, *75*, 174506. [CrossRef]
32. Biškup, N.; Das, S.; Gonzalez-Calbet, J.M.; Bernhard, C.; Varela, M. Atomic-resolution studies of epitaxial strain release mechanisms in $La_{1.85}Sr_{0.15}CuO_4/La_{0.67}Ca_{0.33}MnO_3$ superlattices. *Phys. Rev. B* **2015**, *91*, 205132. [CrossRef]
33. Dragomir, M.; Ma, Q.; Clancy, J.P.; Ataei, A.; Dube, P.A.; Sharma, S.; Huq, A.; Dabkowska, H.A.; Taillefer, L.; Gaulin, B.D. Materials preparation, single-crystal growth, and the phase diagram of the cuprate high-temperature superconductor $La_{2-x}Sr_xCuO_4$. *Phys. Rev. Mater.* **2020**, *4*, 114801. [CrossRef]
34. Dzero, M.; Schmalian, J.; Wolynes, P.G. *Structural Glasses and Supercooled Liquids: Theory, Experiment, and Applications*; Wolynes, P.G., Lubchenko, V., Eds.; Wiley: Hoboken, NJ, USA , 2012; pp. 193–222. [CrossRef]